Enhancement of peroxidase activity in the artificial Mimochrome VI catalysts through rational design.

Giorgio Caserta,[+][a],[b] Marco Chino,[+][a] Vincenzo Firpo,[a] Gerardo Zambrano,[a] Linda Leone,[a] Daniele D'Alonzo,[a] Flavia Nastri,[a] Ornella Maglio,[a],[c] Vincenzo Pavone[a] and Angela Lombardi*[a]

Abstract: Rational design provides an attractive strategy to tune and control the reactivity of bioinspired catalysts. While there has been considerable progress in the design of heme oxidase mimetics with active site environments of ever-growing complexity and catalytic efficiency, their stability during turnover is still an open challenge. Here we show that the simple incorporation of two 2-amino isobutyric acids into an artificial peptide-based peroxidase resulted in a new catalyst (Fe^{III}-MC6*a), with higher resistance against oxidative damage, and higher catalytic efficiency. A two-fold enhancement of the turnover number, respect to its predecessor, was observed. These results point out the protective role exerted by the peptide matrix and pave the way to the synthesis of robust bioinspired catalysts.

Oxygen activating heme enzymes catalyze a wide range of reactions with high selectivity and catalytic efficiency.[1–3] Side reactions, if any, are reduced to a minimum due to the role of the protein matrix, which regulates the substrate access/release.
Inspired by Nature, significant interest has grown in the last decades in preparing catalysts in which the activity is modulated by second-sphere interactions.[4–10] These interactions may tune the redox potential,[11–14] induce substrate/product specificity,[15–18] and/or assist with proton and electron transfer to and from the metal center.[19–22] The outer-sphere environment is also effective in protecting the catalyst against oxidative damage.[5,6,23]
In order to tackle this challenge, we developed heme-protein mimetics (Mimochromes) by structure-based design.[24–32] Through a miniaturization process, we embedded the metalloporphyrin into a small peptide scaffold, and systematically screened the effect of amino acid substitutions on function.[30,31] Iron(III)-Mimochrome VI (Fe^{III}-MC6) shows peroxidase activity, by mimicking features seen in the first and second coordination spheres of natural heme-peroxidases. Its structure consists of two short peptide chains covalently bound to deuteroporphyrin through its propionic acid functionalities. A tetradecapeptide (*TD*) chain bears the His axial proximal ligand, and a decapeptide (*D*) chain, lacking the metal coordinating residue, creates a substrate binding pocket on the heme distal side. In earlier studies we have demonstrated that both chains modulate the peroxidase activity in this artificial catalyst. One mutation, specifically E^2L in the *(TD)* chain, led to a MC6 analog (herein referred as MC6*), with a four-fold increase in the catalytic efficiency.[31] Removal of the entire distal *(D)* chain causes rapid bleaching of the catalyst, resulting in a much lower turnover number (TON) of the MC6 mono-adduct respect to MC6.[30,31]
Herein we show that two rationally designed simple mutations in the distal *(D)* chain of catalyst MC6* produce a more robust and active catalyst. Taking advantage of our knowledge in the use of non-coded α-amino acids as conformational constraints, we selected 2-amino isobutyric acid (Aib, U), the simplest $C^{\alpha,\alpha}$-disubstituted amino acid, to reduce backbone flexibility in the *(D)* chain, and favor the helical folding.[33–35] In order to find the best positions for Aib mutation in the (*D*) sequence, we performed an *in silico* scan, based on the amino acid helix-forming tendencies.[36] Five positions were excluded from the screening: (i) Asp^1 for its N-capping role; (ii) Glu^2 and Arg^{10} for their contribution to catalysis;[30,31] (iii) Ser^6 as it faces the distal side, where hydrogen peroxide can be accommodated and activated; (iv) Lys^9 as it is required to covalently bind the porphyrin. Four out of the eight possible sequences (with non-contiguous Aib residues) gave the best scores (see ESI, Table S1). The sequence containing the Q^3U and S^7U mutations was selected as the *(D)* chain of the new analog, named MC6*a.

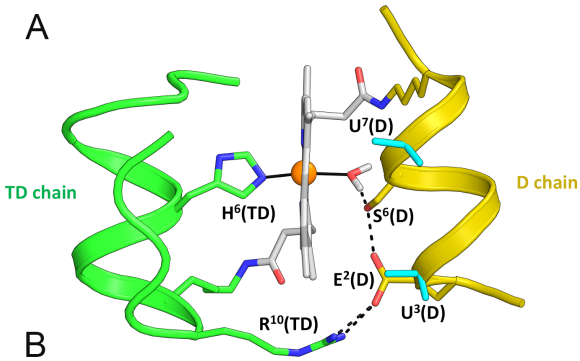

TD chain	**MC6*=MC6*a**	Ac-D-**L**-Q-Q-L-H-S-Q-K-R-K-I-T-L-NH_2
D chain	**MC6***	Ac-D-E-Q-Q-L-S-S-Q-K-R-NH_2
	MC6*a	Ac-D-E-**U**-Q-L-S-**U**-Q-K-R-NH_2

Figure 1. (A) MC6*a designed model. Backbone is represented as ribbon. *(D)* and *(TD)* chains are depicted in gold and in green, respectively. Functional and structural residues are represented as sticks, and iron ion as orange ball. (B) Amino acid sequences of MC6*a and its predecessor MC6* (mutated residues are highlighted in cyan).

[a] *Dr. G. Caserta,[+] Dr. M. Chino,[+] Dr. V. Firpo, Dr. G. Zambrano, Dr. L. Leone, Dr. D. D'Alonzo, Prof. F. Nastri, Prof. V. Pavone, Prof. A. Lombardi*
Department of Chemical Sciences, University of Naples "Federico II"
via Cintia, 80126, Napoli (Italy)
E-mail: alombard@unina.it

[b] *Dr. G. Caserta (present address)*
Department of Chemistry, Technische Universität, Berlin
Straße des 17 Juni, 135, 10623, Berlin (Germany)

[c] *Dr. O. Maglio*
IBB, National Research Council
Via Mezzocannone 16, 80134, Napoli (Italy)

[+] *These authors contributed equally to this work.*
Supporting information for this article is given via a link at the end of the document.

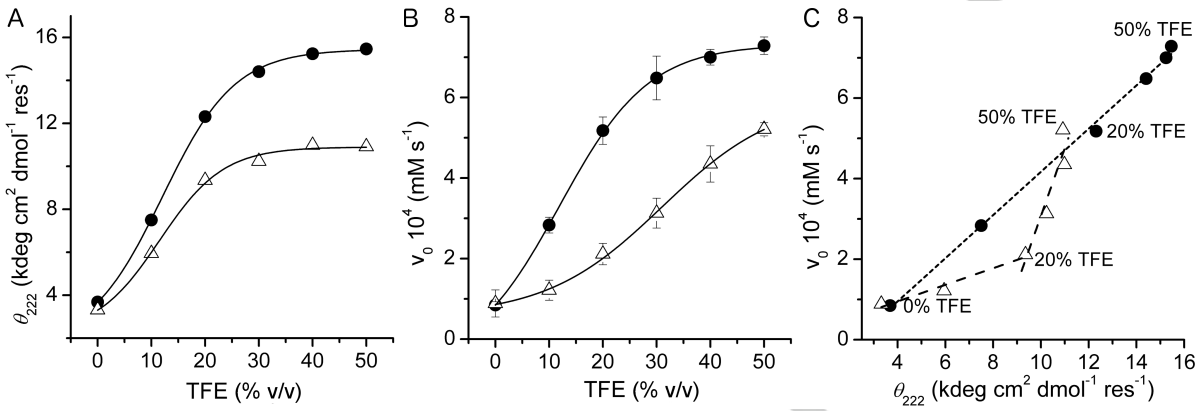

Figure 2. Helical propensity and catalytic performance for Fe^{III}-MC6*a (filled circles) and Fe^{III}-MC6* (open triangles). (A) θ_{222} nm as a function of TFE concentration. (B) Initial rate of ABTS oxidation as a function of TFE (phosphate buffer 50 mM pH 6.5, variable TFE concentration (% *v/v*)). (C) Initial rate of ABTS oxidation as a function of the normalized θ_{222} as measured at different TFE concentrations. See Supporting Information for experimental details.

Positions 3 and 7 (*i, i+4*) place the two Aib residues on the same face of the helix. According to our model, only mutations at such positions allow both Aib side chains to face towards the porphyrin, thus stabilizing the global sandwich topology (see ESI, and Figures 1, S1 and S2). As a consequence, the selected mutations should protect deuteroheme against oxidative damage, and enhance the catalyst peroxidase activity.

MC6*a was synthesized as previously described (see Figures S3-S10, and ESI for synthetic details).[31] The synthesis of the two peptides on a medium-scale (20 mmol) afforded the products in high yields (≈ 85%). This sustains the feasibility of scaling-up the MC6*a synthesis , for future industrial and biotechnological applications.[37]

UV-Vis and CD spectroscopies were combined to analyze the Fe^{III}-MC6*a structural features. As expected Aib mutations in the Fe^{III}-MC6*a *(D)* chain do not significantly alter the heme-coordination state of the new catalyst with respect to Fe^{III}-MC6*. In fact, the UV/Vis spectra of the two catalysts, collected in the same experimental conditions, are almost superimposable, and representative of a 6-coordinate His-H_2O species. The UV/Vis spectral data suggest a high spin state for both complexes (Figure S11).

In 50 mM phosphate buffer (pH 6.5), the CD spectrum of Fe^{III}-MC6*a is reminiscent of an α-helix secondary structure, with a slight increase in helix content respect to Fe^{III}-MC6* (Figure S12 and Table S2). Addition of the helix-inducing solvent 2,2,2-trifluoroethanol (TFE)[38] revealed marked differences between the two catalysts. For both analogs, the α-helical content increases upon TFE addition in amounts up to 50% (*v/v*) (Figure 2A). Interestingly, enhanced helicity, as determined by the intensity of the molar ellipticity at 222 nm (θ_{222}), is observed for the new analog at each TFE contents (Figure 2A*)*. As reported by Roccatano et al,[39] TFE acts on a preexisting helix-coil equilibrium. Due to its preferential solvation for the folded state, TFE interactions with the folded state shift the equilibrium toward the more structured conformation. In the presence of Aib residues, a lower TFE content, respect to the parent analogue, is needed to enhance folding. This finding indicates that the two Aib mutations strongly influence the helical propensity of the (D) peptide chain, as predicted (Figures 2A and S12, Table S2).

To test whether the Aib-containing *(D)* chain affects the catalysis, the oxidation of the 2,2'-azino-bis(3-ethylbenzothiazoline-6-sulphonic acid) (ABTS) in the presence of H_2O_2 was assayed.

First, the effect of the pH and TFE concentration on the catalytic performance was studied. As already observed for Fe^{III}-MC6*, the pH profile of the initial rate (v_0) showed a bell-shaped curve, with a maximum at pH 6.5 (Figure S15). This behavior cannot be related to pH-induced changes in Fe^{III}-MC6*a structure, as the far-UV CD spectra, in the pH range 4.5-7.5, are quite superimposable (Figure S13).

For both analogs, the v_0 is strongly influenced by TFE (Figure 2B). Comparing the two curves, it clearly appears that the presence of Aib residues in the *(D)* chain has a positive effect on catalysis, and nicely correlates with the higher Fe^{III}-MC6*a helical propensity. Fe^{III}-MC6*a overcomes Fe^{III}-MC6* in the v_0 value, at each TFE content. Remarkably, at 20% TFE, the v_0 value of the ABTS oxidation shows a 2.5-fold enhancement when catalyzed by Fe^{III}-MC6*a respect to Fe^{III}-MC6*. Further, the maximum v_0 value reached by Fe^{III}-MC6* at 50% TFE is matched by Fe^{III}-MC6*a at just 20% TFE.

Figure 2C reports a plot of v_0 *vs* θ_{222} at different TFE concentrations for Fe^{III}-MC6*a and Fe^{III}-MC6*. In Fe^{III}-MC6*a, catalytic activity linearly correlates with θ_{222} (Figure 2C, filled circles). Two linear dependences of v_0 *vs* θ_{222}, with different slopes, were instead observed for Fe^{III}-MC6* in the 0–20% and 20–50% TFE regions (Figure 2B, open triangles). By assuming that the catalytic performances of Mimochromes are not only related to the peptide chain helical content but rather to the overall structural topology,[30–32] we propose that the low increase in the v_0 value up to 20%, observed for Fe^{III}-MC6*, only correlates with the random coil ↔ helix transition of the peptide chains.

Enzyme	K_M H_2O_2 (mM)	K_M ABTS (10^{-2}mM)	k_{cat} (10^3 s^{-1})	k_{cat}/K_M H_2O_2 ($10^3 mM^{-1}s^{-1}$)	k_{cat}/K_M ABTS ($10^3 mM^{-1}s^{-1}$)	TON (10^{-3})
Fe^{III}-MC6*	130±20	5.0±0.6	2.3±0.2	0.018±0.003	46±7	5.9
Fe^{III}-MC6*a	440±50	9±1	5.8±0.3	0.013±0.002	64±8	14
HRP	0.93±0.05	70±8	2.70±0.03	2.9±0.2	3.8±5	50

Experimental conditions are given in detail in the Supporting Information

At higher TFE concentrations, the helical folding necessary for driving the *(D)* chain on the porphyrin is reached, and a well-defined sandwiched structure is stabilized. This may account for the higher increase in the v_0 value observed from 20 to 50%. For Fe^{III}-MC6*a, Aib residues exert a favorable effect in driving folding of the *(D)* chain on the porphyrin and in stabilizing the global sandwiched topology, even at low TFE content. This explains the observed v_0/θ_{222} correlation. The stabilization of the sandwiched topology by Aib residues is also supported by CD spectra in the Soret region (Figure S14). The induced Cotton effect is more intense for Fe^{III}-MC6*a respect to Fe^{III}-MC6*, thus indicating a stronger interaction between the porphyrin and the peptide chains in the former catalyst, as already observed for other mimochrome analogues.[25,26,31]

Catalytic parameters were determined by stopped-flow techniques for both Fe^{III}-MC6* and Fe^{III}-MC6*a (Table 1 and Figure S16). The turnover frequency k_{cat} showed a 2.5-fold increase compared to Fe^{III}-MC6* and overcame the natural horseradish peroxidase in the oxidation of ABTS. However, Fe^{III}-MC6*a and Fe^{III}-MC6* showed similar catalytic efficiencies (k_{cat}/K_M) for both H_2O_2 and ABTS, because of the increase in K_M. This can be interpreted in terms of access to the active site, which is narrowed by the Aib-containing (*D*) chain, facing the heme substrate-binding site. The reduced hydrophilicity on the distal side, caused by the Aib methyl substituents, may also account for the observed higher K_M value for H_2O_2.

The kinetic parameters reported in Table 1 confirm and remind us that HRP is evolved for the reduction of hydroperoxides, due to its binding pocket able to properly accommodate H_2O_2. Conversely, MC6*a has a higher affinity for the reducing co-substrates, such as ABTS. As a consequence, HRP remains the most efficient catalyst for the reduction of H_2O_2, whereas its Mimochrome mimics, in particular MC6*a, are the most efficient catalysts for the transformation of ABTS, relatively to HRP and other designed peroxidase catalysts (Table S3).

Notably, Fe^{III}-MC6*a presents a two-fold increase of the TON, respect to its predecessor. The minimum concentration of Fe^{III}-MC6*a, needed to convert 0.10 mM ABTS with an excess of hydrogen peroxide (3.0 mM), was found to be 7.0 nM, corresponding to 14,000 turnovers (Figure S17).

Fitting of the experimental data with a simple pseudo-first-order kinetic model indicates absence of bleaching for Fe^{III}-MC6*a (Figure 3A). Conversely, incomplete ABTS conversion was observed when Fe^{III}-MC6* was used as catalyst at 7.0 and 10.0 nM concentrations, under the same experimental conditions, thus demonstrating unspecific catalyst degradation (Figure 3B).

Because of the established relationship between the TON and the protective role of the (*D*) chain,[30] these data strongly support the hypothesis that Aib residues drive the fold of the new catalyst and, as a consequence, increase its robustness.

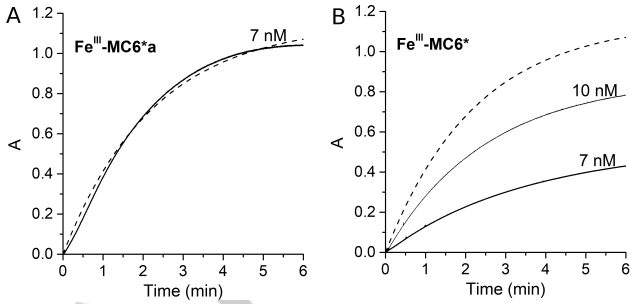

Figure 3. ABTS oxidation, as followed at 660 nm, catalyzed by 7.0 nM (**2**) (A solid line) and by 7.0 and 10 nM (**1**) (B solid line). Dashed line curves simulate the complete ABTS oxidation considering a pseudo-first order kinetic model.

We expect that the hydrophobic patch formed by the Aib methyl groups and the porphyrin might be key to the observed enhanced activity/stability toward catalyst degradation. This hypothesis is supported by preliminary NMR analysis (data not shown) on the diamagnetic Co^{III} derivative of MC6*a. Both, U^3 and U^7 methyl groups experience ring current shielding effect, exhibiting chemical shift values lower than the average reported in BMRB Database ($\Delta\delta$ = 0.1-0.2ppm).[40]

In designing Fe^{III}-MC6*a, the goal was to enhance the functional properties of a synthetic peroxidase through minimal peptide sequence mutation. Through incorporation of two helix-inducing Aib residues, Fe^{III}-MC6*a exceeds the turnover frequency and the total turnover number of its best predecessor.

In conclusion, we have herein demonstrated that a properly designed folded peptide scaffold around the active site may be a route to enhance the catalytic performances of the heme center, and the TON. These results constitute an important step toward understanding how to engineer novel bio-catalysts that are active and robust.

Acknowledgements

The authors wish to thank Fabrizia Sibillo for technical assistance. This work has been supported the European Union (EU) (Cost Action CM1003 - Biological Oxidation Reactions: Mechanisms and Design of New Catalysts) and the Scientific Research Department of Campania Region (BIP Project, POR FESR 2007/2013, grant number B25C13000290007, and STRAIN Project, grant number B25B0900000000, postdoctoral fellowship to M. C.).

Keywords: Heme-protein models • Artificial peroxidases • Non-coded amino acids • Oxidation catalysis • Protein design

[1] T. L. Poulos, *Chem. Rev.* **2014**, *114*, 3919–3962.
[2] O. Maglio, F. Nastri, A. Lombardi, in *Ionic Interactions in Natural and Synthetic Macromolecules* (Eds.: A. Ciferri, A. Perico), John Wiley & Sons, Inc., Hoboken, NJ, USA, **2012**, pp. 361–450.
[3] L. Reisky, H. C. Büchsenschütz, J. Engel, T. Song, T. Schweder, J.-H. Hehemann, U. T. Bornscheuer, *Nat. Chem. Biol.* **2018**, *14*, 342–344.
[4] S. Sahu, D. P. Goldberg, *J. Am. Chem. Soc.* **2016**, *138*, 11410–11428.
[5] M. Chino, L. Leone, G. Zambrano, F. Pirro, D. D'Alonzo, V. Firpo, D. Aref, L. Lista, O. Maglio, F. Nastri, et al., *Biopolymers* **2018**, DOI 10.1002/bip.23107.
[6] X. Huang, J. T. Groves, *Chem. Rev.* **2018**, *118*, 2491–2553.
[7] K. Oohora, T. Hayashi, *Methods Enzymol.* **2016**, *580*, 439–454.
[8] C. P. S. Badenhorst, U. T. Bornscheuer, *Trends Biochem. Sci.* **2018**, *43*, 180–198.
[9] C. J. Reedy, B. R. Gibney, *Chem. Rev.* **2004**, *104*, 617–650.
[10] O. Iranzo, *Bioorg. Chem.* **2011**, *39*, 73–87.
[11] J. Liu, S. Chakraborty, P. Hosseinzadeh, Y. Yu, S. Tian, I. Petrik, A. Bhagi, Y. Lu, *Chem. Rev.* **2014**, *114*, 4366–4469.
[12] I. Batinic-Haberle, A. Tovmasyan, I. Spasojevic, *Redox Biol.* **2015**, *5*, 43–65.
[13] S. Shinde, J. M. Cordova, B. W. Woodrum, G. Ghirlanda, *J. Biol. Inorg. Chem.* **2012**, *17*, 557–564.
[14] J. G. Kleingardner, K. L. Bren, *Acc. Chem. Res.* **2015**, *48*, 1845–1852.
[15] S. C. Hammer, G. Kubik, E. Watkins, S. Huang, H. Minges, F. H. Arnold, *Science* **2017**, *358*, 215–218.
[16] J.-P. Mahy, J.-D. Maréchal, R. Ricoux, *Chem. Commun.* **2015**, *51*, 2476–2494.
[17] J.-P. Mahy, J.-D. Maréchal, R. Ricoux, *J. Porphyr. Phthalocya.* **2014**, *18*, 1063–1092.
[18] M. Kryjewski, T. Goslinski, J. Mielcarek, *Coord. Chem. Rev.* **2015**, *300*, 101–120.
[19] T. A. Farid, G. Kodali, L. A. Solomon, B. R. Lichtenstein, M. M. Sheehan, B. A. Fry, C. Bialas, N. M. Ennist, J. A. Siedlecki, Z. Zhao, et al., *Nat. Chem. Biol.* **2013**, *9*, 826–833.
[20] D. W. Watkins, J. M. X. Jenkins, K. J. Grayson, N. Wood, J. W. Steventon, K. K. L. Vay, M. I. Goodwin, A. S. Mullen, H. J. Bailey, M. P. Crump, et al., *Nat. Commun.* **2017**, *8*, 358.
[21] M. Faiella, O. Maglio, F. Nastri, A. Lombardi, L. Lista, W. R. Hagen, V. Pavone, *Chem. Eur. J.* **2012**, *18*, 15960–15971.
[22] L. A. Solomon, J. B. Kronenberg, H. C. Fry, *J. Am. Chem. Soc.* **2017**, *139*, 8497–8507.
[23] J. P. Klinman, *Acc. Chem. Res.* **2007**, *40*, 325–333.
[24] F. Nastri, M. Chino, O. Maglio, A. Bhagi-Damodaran, Y. Lu, A. Lombardi, *Chem. Soc. Rev.* **2016**, *45*, 5020–5054.
[25] G. D'Auria, O. Maglio, F. Nastri, A. Lombardi, M. Mazzeo, G. Morelli, L. Paolillo, C. Pedone, V. Pavone, *Chem. Eur. J.* **1997**, *3*, 350–362.
[26] A. Lombardi, F. Nastri, D. Marasco, O. Maglio, G. De Sanctis, F. Sinibaldi, R. Santucci, M. Coletta, V. Pavone, *Chem. Eur. J.* **2003**, *9*, 5643–5654.
[27] L. Di Costanzo, S. Geremia, L. Randaccio, F. Nastri, O. Maglio, A. Lombardi, V. Pavone, *J. Biol. Inorg. Chem.* **2004**, *9*, 1017–1027.
[28] C. Vicari, I. H. Saraiva, O. Maglio, F. Nastri, V. Pavone, R. O. Louro, A. Lombardi, *Chem. Commun.* **2014**, *50*, 3852–3855.
[29] A. Ranieri, S. Monari, M. Sola, M. Borsari, G. Battistuzzi, P. Ringhieri, F. Nastri, V. Pavone, A. Lombardi, *Langmuir* **2010**, *26*, 17831–17835.
[30] F. Nastri, L. Lista, P. Ringhieri, R. Vitale, M. Faiella, C. Andreozzi, P. Travascio, O. Maglio, A. Lombardi, V. Pavone, *Chem. Eur. J.* **2011**, *17*, 4444–4453.
[31] R. Vitale, L. Lista, C. Cerrone, G. Caserta, M. Chino, O. Maglio, F. Nastri, V. Pavone, A. Lombardi, *Org. Biomol. Chem.* **2015**, *13*, 4859–4868.
[32] R. Vitale, L. Lista, S. Lau-Truong, R. T. Tucker, M. J. Brett, B. Limoges, V. Pavone, A. Lombardi, V. Balland, *Chem. Commun.* **2014**, *50*, 1894–1896.
[33] R. Banerjee, G. Basu, *ChemBioChem* **2002**, *3*, 1263–1266.
[34] Karle I. L., *Pept. Sci.* **2004**, *60*, 351–365.
[35] B. Di Blasio, V. Pavone, A. Lombardi, C. Pedone, E. Benedetti, *Biopolymers* **2004**, *33*, 1037–1049.
[36] K. T. O'Neil, W. F. DeGrado, *Science* **1990**, *250*, 646–651.
[37] V. Pavone, F. Nastri, O. Maglio, A. Lombardi, *High-Efficiency Catalysts, Preparation and Use Thereof*, **2011**, 20130244232 A1.
[38] D.-P. Hong, M. Hoshino, R. Kuboi, Y. Goto, *J. Am. Chem. Soc.* **1999**, *121*, 8427–8433.
[39] D. Roccatano, G. Colombo, M. Fioroni, A. E. Mark, *Proc. Natl. Acad. Sci. U.S.A.* **2002**, *99*, 12179–12184.
[40] D. Labudde, D. Leitner, M. Krüger, H. Oschkinat, *J. Biomol. NMR* **2003**, *25*, 41–53.

Entry for the Table of Contents

Layout 1:

COMMUNICATION

The simple incorporation of two helix-inducing Aib residues into an artificial peptide-based peroxidase enhances its robustness and efficiency.

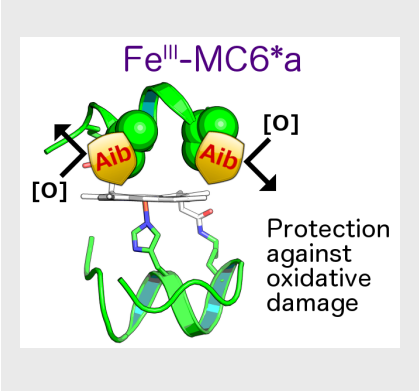

*Giorgio Caserta, Marco Chino, Vincenzo Firpo, Gerardo Zambrano, Linda Leone, Daniele D'Alonzo, Flavia Nastri, Ornella Maglio, Vincenzo Pavone and Angela Lombardi**

Page No. – Page No.

Enhancement of peroxidase activity in the artificial Mimochrome VI catalysts through rational design.